Chapter 4

Dynamic light scattering studies of some modes with wavevectors perpendicular to the twist axis in cholesterics

4.1 Introduction

In the previous chapter, we described our studies on a well isolated viscoelastic mode with wavevector parallel to the twist axis in a cholesteric. Those experiments were performed in the back scattering arrangement. In this chapter, we study fluctuations with wavevectors perpendicular to the twist axis. Here, the associated modes are very different. The experiments were performed in the transmission arrangement, where the light scattered in the forward direction is analyzed. The interesting result we obtain is that at high scattering wavevectors (equivalently scattering angles), the intensity autocorrelation functions have a non-exponential decay, which implies coupled modes. At low scattering wavevectors they turn out to be single exponential suggesting an isolated relaxation mode [1].

4.2 The forward scattering arrangement

In this arrangement, light is incident in a direction normal to the sample cell. The incident light is linearly polarized with its electric vector perpendicular to the scattering plane. In our experiment, the cholesteric sample is aligned with its twist axis parallel to the cell normal. In forward scattering, light is incident in a direction

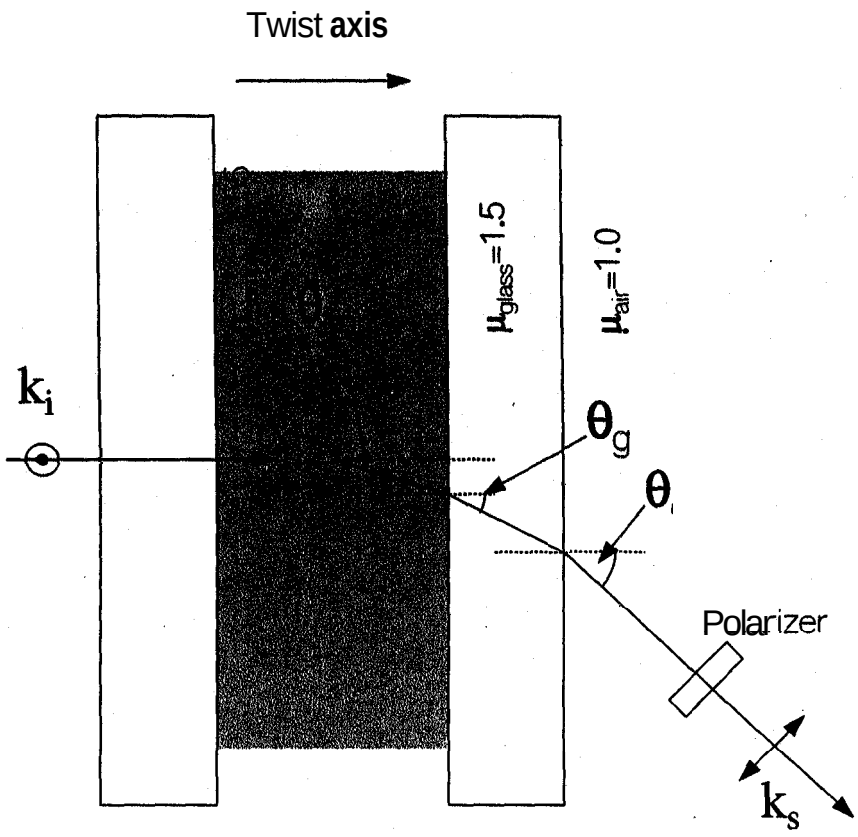

Figure 4.1: Ray diagram showing the interfaces at which the scattered light experiences refraction.In the figure, ⊙ shows that the incident electric vector is perpendicular to the scattering plane while ↔ indicates that the scattered light is analyzed with its electric vector parallel to the scattering plane,

parallel to the twist axis of the cholesteric and the light scattered in the forward direction is analyzed. The scattered light is passed through an analyser (who's axis is parallel to the scattering plane) before it enters the detector. This is known as the VH arrangement. V (vertical) stands for the polarization of the incident light and H (horizontal) for the direction in which the scattered light is analysed. The directions H and V are with reference to the scattering plane.

In these experiments we used a sample holder kept directly in the oven. In the absence of a refractive index matching medium, it is necessary to apply a correction to the observed angle (θ_{obs}) of scattering. This is shown in figure(4.1). In our calculations of the scattering wavevectors, we have used such a corrected scattering angle (θ_{cor}).

The relation between the observed and the corrected angles is given by

$$\theta_{cor} = sin^{-1}\left(\frac{\mu_{air}}{\mu_{sample}} sin(\theta_{obs})\right) \tag{4.1}$$

Here, μ_{air} is the refractive index of air and μ_{sample} is the average refractive index of the sample. The average refractive index of the sample is nearly 1.55.

The details of the scattering arrangement are shown in figure(4.2). A simple geometric analysis yields the following expressions for the components of the scattering wavevector q.

$$q_{\|} = |\mathbf{q}| sin(\theta_{cor}/2)$$

and

$$q_{\perp} = |\mathbf{q}| cos(\theta_{cor}/2)$$

Here, the parallel and perpendicular directions are defined with respect to the twist axis of the cholesteric.

4.3 Experimental

4.3.1 Sample preparation

The cholesteric used in the experiment was a three component mixture consisting of cholesteryl chloride (CCL), cholesteryl nonanoate (CNN) and cholesteryl oleyl carbonate (COC). In the particular mixture used in the experiment, the weight percentages of the compounds were the same as that mentioned in chapter 3. This mixture is a room temperature cholesteric. The cholesteric samples are aligned with the twist axis perpendicular to the glass plate. The details of the alignment procedure and sample preparation have already been described in chapter 3.

4.3.2 Design of the sample cell temperature control unit

To do experiments in the forward scattering arrangement, we constructed a different temperature control unit consisting of two parts, the sample oven and a sample holder. The cholesteric sample cell is mounted on the holder which is housed inside an oven.

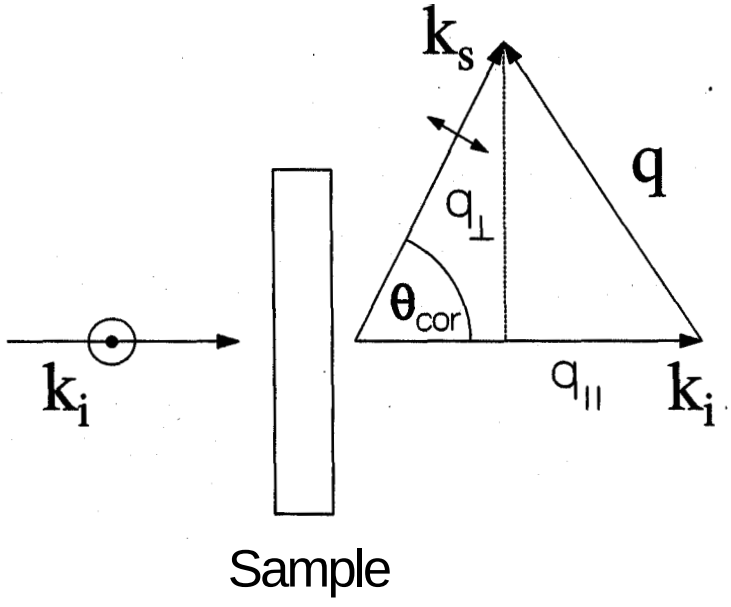

Figure 4.2: The forward scattering arrangement. Here, the sample is aligned such that the twist axis is parallel to the cell normal. The incident wavevector is parallel to the twist axis of the cholesteric and the scattering wavevector is predominantly perpendicular to the twist axis. The VH arrangement is indicated in the figure by the symbols $\odot$ and $\leftrightarrow$ respectively.

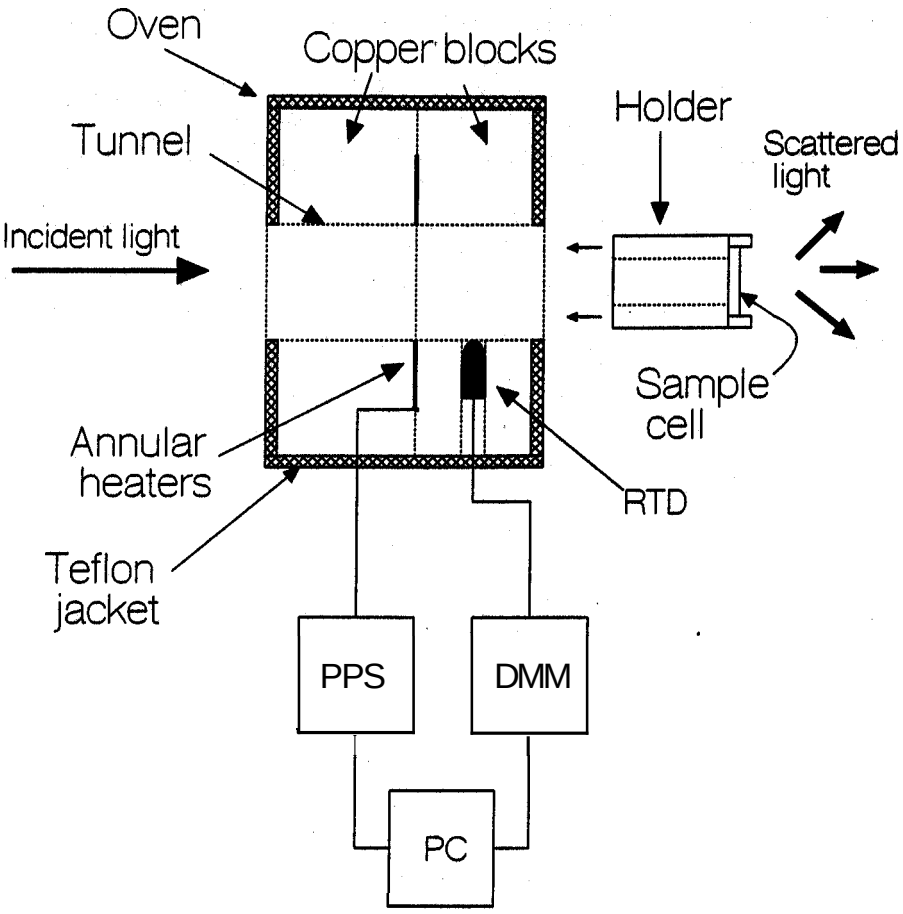

Figure 4.3: A schematic diagram of the oven and sample holder used for the forward scattering experiments. A cross-sectional view from above is shown. DMM is a digital multimeter that measures the RTD resistance. PPS is a programmable power supply that provides power to the heating elements. PC is a personal computer that controls the multimeter and the power supply via a **GPIB** interface.

The oven used in this experiment was designed for good temperature stability and hence had a large thermal mass. A schematic diagram of the sample oven and holder is shown in figure(4.3).

The oven consists of two blocks of copper firmly bolted together with the heating elements (Kapton type, Minco Inc.) sandwiched between them. Each of the two blocks had a central cylindrical tunnel in it to accommodate the sample holder and allow the passage of incident and scattered light. The heating elements were annular in shape. The central annulus was exactly of the same diameter as the tunnels in the copper blocks. The heating elements were mounted such that they encircle the tunnel. The advantage of using annular heating elements is that the sample would

be uniformly heated from all sides. This would prevent any temperature gradients across the sample. A small amount of heat sink material was smeared on to the two sides of the heating elements to ensure good thermal contact with the copper blocks. The holder was cylindrical in shape and was also made of copper. The diameter of the holder was almost exactly the same as that of the tunnel. The holder fits snugly in the tunnel to ensure efficient conduction of heat from the oven to the holder. The holder itself has a hole running through its entire length to allow for the passage of the incident light. The sample cell was mounted on the holder with the aid of two metallic screws and was held firmly in contact with the body of the holder with teflon washers. A resistance temperature device (RTD) was positioned such that after mounting the sample, the RTD could be made to slide and come in direct contact with the sample cell. The entire oven was enclosed in a 3mm thick teflon jacket to reduce radiative heat loss. The PI temperature controller described in chapter 2 was used in conjunction with this heater. The experiments described in this chapter were carried out for samples maintained at 32f 0.05°C. The body of the oven was designed with flat outer surfaces so that it could be removed from the goniometer stand and placed on the stage of a polarizing microscope directly. This feature of the oven enabled us to examine the sample alignment between different runs in the light scattering experiments without having to remove the sample cell from the oven.

4.3.3 Apparatus and measurements

Light from a 488 nm Argon ion laser (Spectra Physies Model 163) is incident in a direction normal to the sample cell. The sample oven is positioned such that the scattering volume lies exactly at the intersection of the goniometer axis and the incident beam. Light scattered from the sample enters a photomultiplier tube (PMT) after passing through an analyser. The PMT is mounted on the movable arm of the goniometer. The signals from the PMT are passed on to a digital autocorrelator (Malvern 4700c) via a pre-amplifier discriminator system fabricated by us described in chapter 2. We selected different delay times depending on the angle at which the

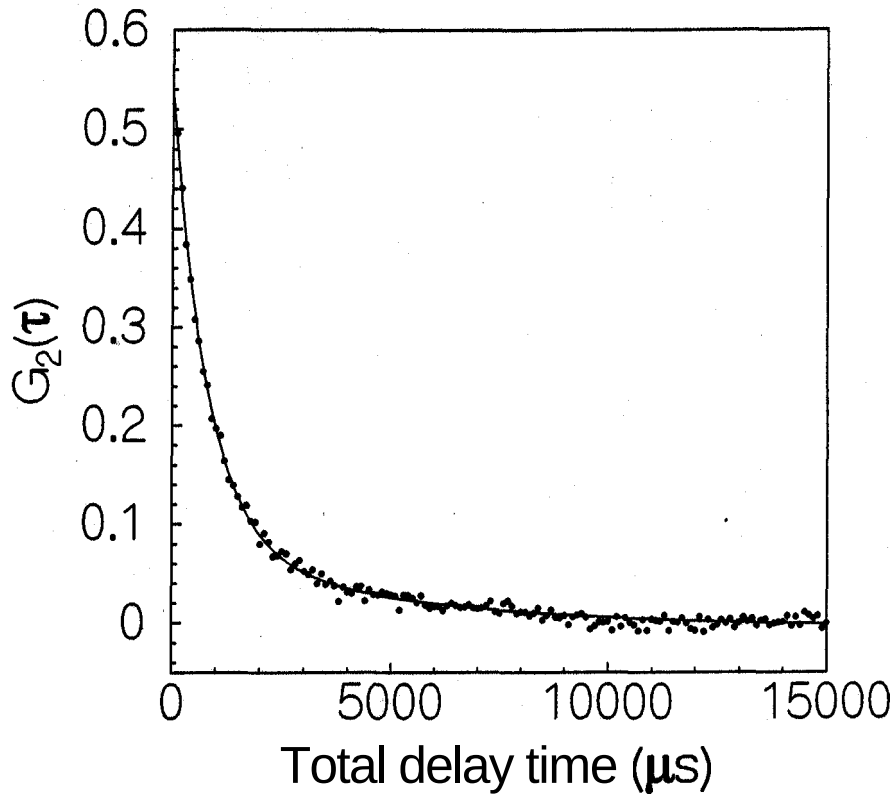

Figure **4.4:** A typical normalized correlogram $G_2(\tau)$, obtained in the experiment. The corrected scattering angle was **29.62** degrees. The sample temperature was maintained at **32f0.05°C.** The delay time was **200** μs and the total integration time was **200s.** The continuous line is obtained from a two exponent relaxation model described in the text.

correlogram data was being acquired. Data was acquired for observed scattering angles between **35** and **50** degrees which corresponded to a range of corrected scattering angles between **29.62** degrees and **21.72** degrees. The total integration time for which each datum was collected was **200** seconds. We observe that the signal to noise ratio of the experiments reduces uniformly as we approach lower scattering angles. At these angles, the signal to noise ratio could be improved by reducing the effective area of the detector by using smaller pinholes. The delay time used is such that the decaying part of the correlation function is recorded in approximately the first **150** channels. The rest of the channels record the tail of the autocorrelation function.

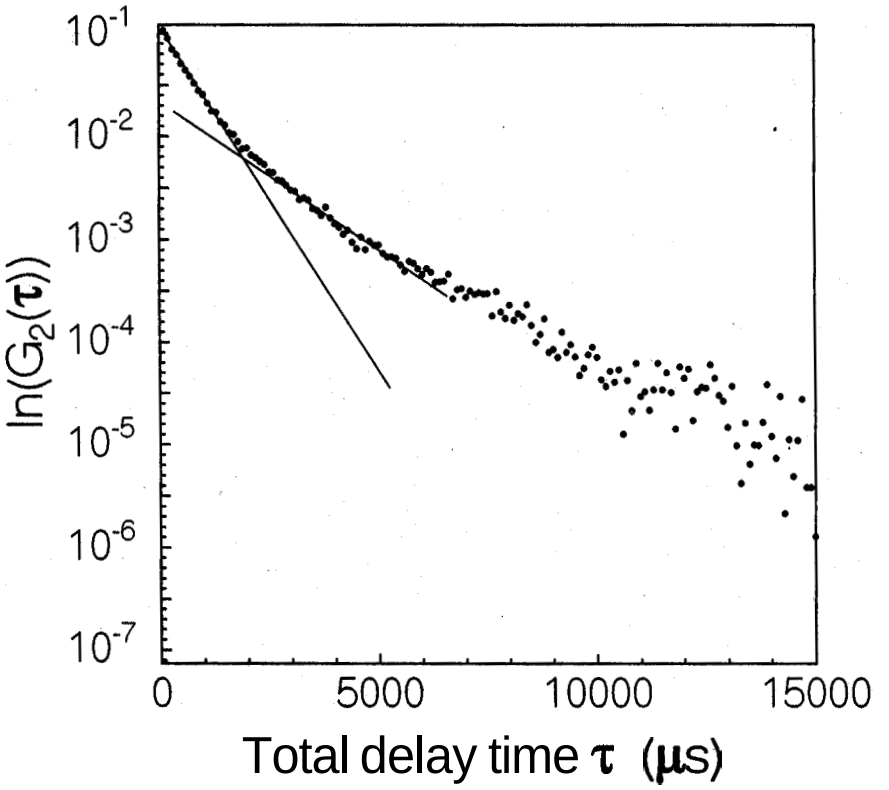

Figure 4.5: The natural logarithm of the intensity correlation function shows a change in slope. There is an initial fast decay and then a slower one. The two slopes correspond to the two time scales present in the fluctuations in the system. The solid lines are drawn as cues to the eye.

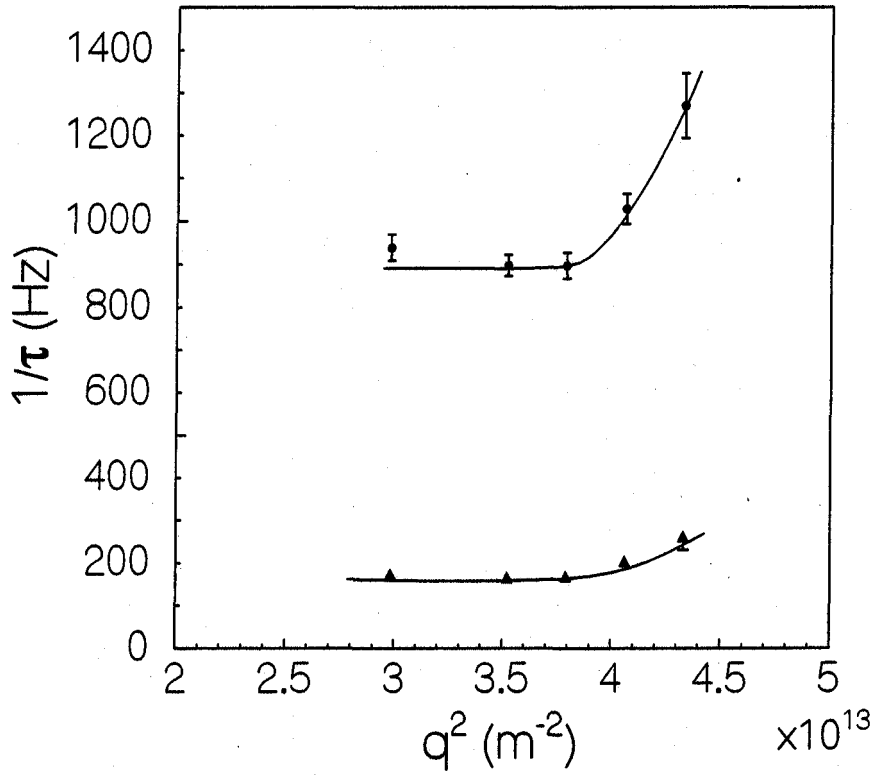

Figure 4.6: The variation of the inverse relaxation times of the two modes obtained in the experiment as a function of the square of the scattering wavevector. The circles indicate the fast mode and the triangles indicate the slow mode. For the slow mode, the error bars are smaller than the size of the markers and hence are not indicated. These experiments were performed at 32±0.05°C. The solid lines are drawn as cues to the eye.

4.4 Analysis of the intensity autocorrelation functions

A typical correlogram obtained in these experiments is shown in figure(4.4). It can be seen that it is not a single exponential decay. We plotted the natural logarithm of the correlation function with the delay time. We could discern two linear portions of different slopes separated by a cross over region. This is shown in figure(4.5). It indicates that there are two relaxation times in the system. Based on this trend, we decided to fit a two exponential decay to our data. The model we have used is,

$$g_2(\tau) = c_1 + c_2 e^{-(\tau/c_3)} + c_4 e^{-(\tau/c_5)} \tag{4.2}$$

Here, c_1 is a base line parameter, c_2 and c_4 are strength parameters and c_3 and c_5 are the relaxation times. We define the normalized autocorrelation function as:

$$G_2(\tau) = \frac{g_2(\tau)}{g_2(\infty)} - 1 = c_2' e^{-(\tau/c_3)} + c_4' e^{-(\tau/c_5)}$$

Where,

$$c_2' = \frac{c_2}{g_2(\infty)}$$

and

$$c_4' = \frac{c_4}{g_2(\infty)}$$

$g_2(\infty)$ is the value of the base line. This value is automatically calculated by the correlator by considering very long delay times.

A fit of our data, the normalized autocorrelation function $G_2(\tau)$, to the two exponential model is shown as a continuous line in figure(4.4). One can notice that the fit is quite good. The error estimates on the relaxation times are calculated from the standard errors obtained by taking five data sets at every angle [2].

4.5 Results and discussions

In the forward scattering arrangement, the scattering wavevector has a large component in a direction perpendicular to the twist axis. This perpendicular component of

the wavevector senses fluctuations within the cholesteric planes. We have detected fluctuations with two distinct time scales.

The inverse relaxation times of these fluctuations as a function of the square of the scattering wavevector are shown in figure(4.6). It can be seen that the two modes behave quite differently. The relaxation time of the faster mode decays rapidly with wavevector and seems to saturate at lower wavevectors [3]. On the other hand, the slower mode doesn't appear to have such a marked dependence on wavevector. We speculate that' we are observing some new coupled modes. These modes might be arising due to the coupling of the twist and umbrella fluctuations. The analysis of these modes is quite complex in this forward scattering arrangment since it is not possible to isolate them.

It is also possible that these modes are due to layer undulations. According to an argument by de Gennes [4] we can assume that at some level of coarse graining, cholesterics and smectics become indistinguishable from each other. This is called the 'jelly roll' model. In this model there can be layer undulations that cause scattering in a direction perpendicular to the twist axis.

More experiments on $g_2(\tau)$ as a function of temperature, pitch, sample thickness and other parameters are necessary to investigate the origin of these coupled modes.

Bibliography

[1] M. S. Veshchunov. *Sov.* Phys. JEPT, 49, 769 (1979).

[2] S. K. Muthu. Probability and Errors for the Physical Sciences. Orient Longman Limited, New Delhi (1982).

[3] T. Harada and P. P. Crooker. Phys. Rev. Lett., 34, 1259 (1975).

[4] P. G. de Gennes and J. Prost. The Physics of Liquid Crystals, 2nd ed., Clarendon press, Oxford, (1993).